Proceedings of Ninth World Conference on Earthquake Engineering
August 2-9, 1988, Tokyo-Kyoto, JAPAN (Vol.IV)

6-3-12

AN EXPERIMENTAL STUDY OF SEISMICALLY RESISTANT ECCENTRICALLY BRACED FRAMES WITH COMPOSITE FLOORS

Egor P. POPOV[1] and James M. RICLES[2]

[1]Department of Civil Engineering,
University of California, Berkeley, California 94720, USA
[2]Department of Applied Mechanics and Engineering Science,
University of California at San Diego, La Jolla, California 92093, USA

SUMMARY

Described are the results of an experimental study on the effects of composite action in seismically resistant eccentrically braced steel frames having a concrete floor slab. The objectives of this study were to assess the cyclic strength and ductility of short composite links, the effectiveness of the floor slab in providing restraint to the links against lateral-torsional buckling, and the participation of the floor beam outside the link.

INTRODUCTION

An eccentrically braced steel frame, EBF, is a structural system in which at least one end of every brace is connected so as to isolate a beam segment called a *link*. During overloading of an EBF the links are designed to act as fuses by yielding and dissipating energy, thereby limiting the amount of force that the adjacent columns and braces must resist. When properly detailed, these links provide a stable source of energy dissipation. Brace buckling is inhibited by designing the brace members to resist the forces associated with the strength of the links. This feature, coupled with the property of large elastic stiffness, make EBFs a very suitable structural system for seismically active regions.

Past research in the U.S. has been devoted to studying the hysteretic properties of bare steel links in order to establish criteria for their design. The first experiments dealing with the seismic response of EBFs with composite floors was that of Phase II of the U.S./Japan cooperative research program conducted in Tsukuba, Japan (Ref.1). The test specimen consisted of a full scale K-braced EBF where the links were located at midspan of the floor beams in the braced bay. Test results indicated that links with composite floors would likely perform well during extreme seismic events. Because of a local failure in a brace-beam connection at extreme cyclic load in the Tsukuba test, and a lack of data on link behavior next to columns, a research program on cyclic behavior of composite links was conducted at Berkeley on an NSF sponsored project (Ref.2). The Tsukuba EBF was used as a prototype structure, where the first floor link where failure occurred was a W18 x 40.

EXPERIMENTAL PROGRAM

Links were tested for K-braced and V-braced EBF configurations using two-thirds scale subassemblies simulating the floor beams shown in Figs. 1(a) and (b). In both frames the plastic link rotation γ_p is related to the plastic story drift angle θ_p, bay width L, and link length e by:

$$\gamma_p = \theta_p L / e \tag{1}$$

The kinematics of the K-braced EBF mechanism in Fig. 1(a) requires that the corresponding subassembly be subjected to equal but opposite displacements δ at the ends of the link, while the V-braced EBF

subassembly requires that the imposed link end displacements result in an equal slope of θ in both beam segments outside the link. The link rotations γ in the subassemblies, neglecting small amount of elastic deformation, correspond reasonably well to γ_p of the EBFs. To account for the exterior column rotational constraint in the V-braced EBF, the beam moment of inertia was increased on one side of the link. The link end displacements δ were imposed by cyclic jack forces P_A and P_B. These forces simulated the vertical components of axial brace force in the K-braced subassembly, and the exterior column axial force and the vertical component of axial force of one of the braces in the V-braced subassembly. The experimental simulation did not consider axial force effects in the link. It is believed, however, that the floor beam moment and shear forces developed in the vicinity of the link corresponded reasonably well to conditions in an EBF.

Tests were performed on six composite and two bare steel link specimens. The composite links were a part of a composite lightweight concrete floor slab of 16 ft. width and 18 ft. length, which was cast on formed metal deck and supported from below by three parallel W12 x 19 steel floor beams, Beams A, B, and C as shown in plan in Fig. 2(a). In this figure the locations of the six composite links are identified. The two bare steel links D1 and D2 are shown on an isolated beam. Eight specimens are identified and described in the first and second columns of Table 1. An elevation of the test setup for a composite link in a K-braced subassembly is shown in Fig. 2(b). By moving the test end frame from location 1 to 6, the pinned column support from location 4 to 2, and the hydraulic jacks from locations 2 to 4 and 3 to 5, a V-braced subassembly was obtained for the same beam. The extent of floor slab damage was expected to be small based on observations during the Tsukuba tests, thereby justifying the use of one floor slab and three floor beams for constructing the six composite specimens.

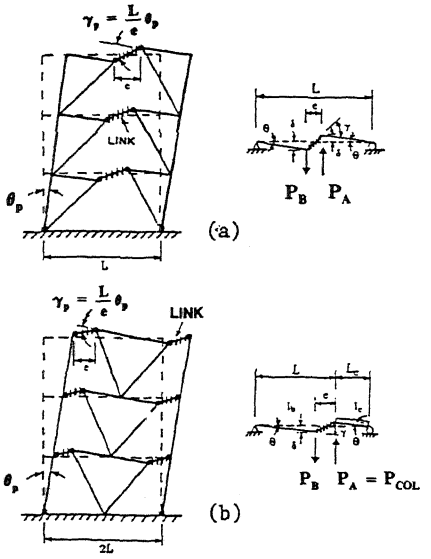

Fig.1 (a)K-Braced, and (b)V-Braced EBFs with Experimental Subassemblies.

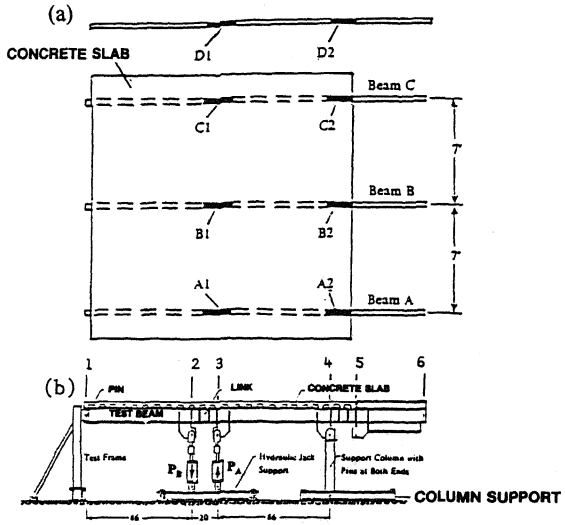

Fig.2 (a)Plan of Specimen Location, and (b)Elevation of K-Braced EBF Subassembly.

The details of the composite floor slab consisted of a standard 20 gage cold formed metal deck with two inch high ribs. The lightweight concrete slab was 4.5 in. thick. The ribs were placed perpendicular to the floor beams. Pairs of shear connectors of 3.5 in. length and 0.5 in. diameter were welded directly through the deck in each rib to the floor beam top flange at a six inch spacing, except along a 12 ft. length centered above Specimen B1, where the metal decking was removed allowing the shear connectors to be placed at a 4 in. spacing. This detail was similar to that in the Tsukuba EBF. The average compressive strength of the lightweight concrete slab during testing was 4200psi. The links were designed to yield in shear based on bare steel criteria and were 19 in. long. One sided web stiffeners were welded to the web and flanges in the link. A stiffener spacing to web thickness ratio, a/t_w, of 25 was used for all composite links, except for Specimen A2 where the stiffener spacing was reduced by one-half resulting in the ratio a/t_w being equal to 12.5. The average yield strength of the W12 x 19 floor beam determined by tension coupon tests was 49.7 ksi, with an average ultimate strength of 64.3 ksi. In all tests except for Specimen

C2, at both ends of the link and at intermediate points outside the link lateral bracing was provided from one side by W10 x 15 beams with simple connections. Specimen C2 was not laterally braced at either end of the link.

Specimen [1]	EBF Type [2]	K* (kips/in) [3]	V_y (kips) [4]	M_y (kip-in) [5]	$\frac{V_y}{V_{yD1}}$ [6]	$\frac{V_y}{V_{yD2}}$ [7]	$\frac{V_y}{V_p}$ [8]	$\frac{M_y}{M_p}$ [9]
A1	Composite Exterior K-Braced	706	88.1	975	1.03	–	0.95	0.82
B1	Composite Interior K-Braced	859	100.1	1154	1.17	–	1.07	0.97
C1	Composite Exterior K-Braced	707	86.9	965	1.02	–	0.92	0.81
D1	Bare Steel K-Braced	569	85.3	1170	1.00	–	0.92	0.98
A2	Composite Exterior V-Braced	747	87.0	1021	–	1.08	0.93	0.86
B2	Composite Interior V-Braced	812	94.7	1182	–	1.16	1.02	0.99
C2	Composite Exterior V-Braced	744	85.9	914	–	1.06	0.92	0.77
D2	Bare Steel V-Braced	698	81.4	1111	–	1.00	0.87	0.93

Table 1 Link Identification, Initial Elastic Stiffness and Force at Initial Yielding of Specimens.

All test specimens were subjected to quasi-static cyclic forces P_A and P_B (see Fig. 1) causing progressively increasing link rotation angles $\pm \gamma$. The maximum magnitudes of these angles were comparable to those that may occur during a major earthquake. The history of γ for all specimens, excluding C1, consisted of a sequence in which the magnitudes of successive pairs of rotation cycles were 0.02, 0.04, 0.06, 0.08, and 0.10 rad. Prior to this sequence of cyclic deformation in Specimens A1 and C2, random pulses of large γ were applied. The history for γ applied to Specimen C1 was based on the measured first floor inter-story drift of the Tsukuba EBF subjected to the Taft earthquake with a peak ground acceleration of 0.5g. In the subassemblies the link displacements were monitored by linear potentiometers at the link ends to measure both the vertical movement and twist of the beam. Rotation at the link ends and the slip between the floor beam and concrete slab were measured using appropriately placed linear variable differential transformers (LVDTs). Hydraulic jack forces and reactions at the ends of the floor beams were monitored using calibrated load cells. The links were whitewashed to aid in observing the pattern and progress of yielding.

EXPERIMENTAL RESULTS

The initial elastic response of each specimen provided data for determining the elastic link stiffness. This pseudo-elastic link stiffness K^* was computed for each specimen by dividing the elastic shear force V by the relative vertical displacement v between the link ends (e.g. $K^* = V/v$). The computed values for K^* are given in the third column of Table 1. These results indicate that all composite links had a greater initial elastic stiffness than the corresponding bare steel links (Specimens D1 and D2), with the interior composite links (Specimens B1 and B2) showing the largest increase. Specimen B1 of the K-braced subassembly has a K^* equal to 1.51 times that of Specimen D1. Since the elastic lateral stiffness of an EBF is influenced by its link stiffnesses, this implies that EBFs with composite floors will have an increased elastic lateral stiffness. In Fig. 3 the shear-deformation, $V - \gamma$, hysteretic loops for the composite link, Specimen B1, have been superimposed onto those of the bare link, Specimen D1 showing the increased initial elastic stiffness of the composite link. However, in subsequent cycles the elastic stiffness of Specimen B1 appears to deteriorate towards that of the bare steel link, Specimen D1. This is a consequence of floor slab damage above the link during the subsequent cycles of link deformation.

In both the bare steel and composite specimens yielding originated in the link webs. Following this yielding, the stiffness of the links decreased dramatically with continued deformation, as shown in Fig. 3. The link shear force V_y at initial yield for all specimens are summarized in column four of Table 1, and are normalized with respect to the bare steel specimens in columns six and seven. Like K^*, V_y are larger for the composite links, particularly for the interior Specimens B1 and B2; their shear strength is also greater than the plastic shear strength $V_p = 0.55\, F_y d t_w$ of the bare steel links (column 8). In column 9 of Table 1 the largest link end moments M_y at initial yield are normalized by the flexural capacity

$M_p = ZF_y$ of a bare steel link. Unlike the shear force, the moment M_y in the composite links is either approximately equal to or less than that of the bare steel links. This is possible because the shear is related to the sum of link end moments, and the sum of the link end moments at initial yield in the composite links exceeded that of the bare steel links. Note that for the composite links M_y does not exceed M_p.

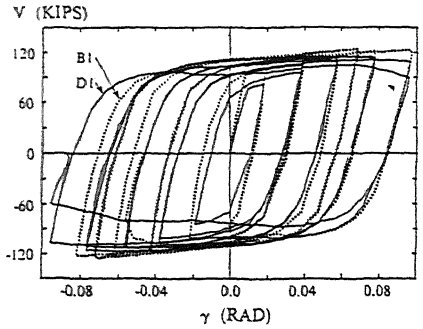

Fig.3 Shear-Deformation Relationship for Composite Specimen B1 and Bare Steel Specimen D1.

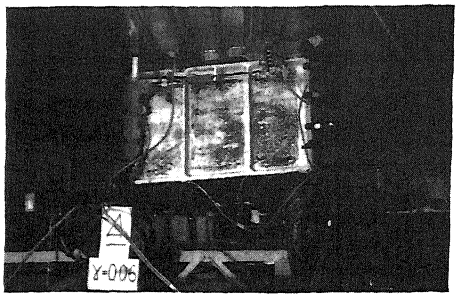

Fig.4 Link of Specimen B1 Prior to Web Buckling with Extensive Web Yielding.

With continued cyclic deformation both the bare steel and the composite links developed extensive web yielding. Furthermore, as shown by the hysteretic loops in Fig. 3, a larger shear force developed in the links in successive cycles is due to combined isotropic and kinematic hardening. However, the discrepancy between their strengths diminishes with the increased number of cycles. Fig. 4 shows the link of Specimen B1 with significant web yielding, evident by the flaked whitewash, and deformed into the shape of a parallelogram at $\gamma = 0.06$ rad. The bare steel links yielded and deformed in a similar manner.

Due to strain hardening the link shear forces increased in successive cycles, until web buckling occurred in the link. Following web buckling the link strength would gradually deteriorate; this effect was more pronounced for the bare steel links. The web stiffeners delayed web buckling and provided a means of developing tension field action in buckled web panels. The deformation of the web stiffeners and flange around the buckled panel shown in Fig. 5 was typical of both the composite and bare steel links following web buckling. The maximum magnitude of link deformation γ_u for bare steel links given in Ref. 3 is

$$a/t_w + d/(5t_w) = C_B \qquad (a \le d) \tag{2}$$

where a, t_w, and d are the stiffener spacing, web thickness, and beam depth, respectively, and the constant C_B = 56, 38, and 29, respectively, for γ_u = 0.03, 0.06, and 0.09 rad. A calculated value of γ_u = 0.072 rad. for the specimens (excluding Specimen A2) agrees reasonably well with measured values of γ_u summarized in column 2 of Table 2. Specimen A2 did not develop web buckling because of the small web stiffener spacing.

A summary of the maximum shear force V_{max} and moment M_{max} developed in the links is given in the third and fourth columns of Table 2. V_{max} of the composite links exceeds that of the bare steel links, where Specimens B1 and B2 developed a V_{max} that was 10 and 11 percent greater than that of Specimens D1 and D2, respectively. Column five of Table 2 gives and indication of the amount of strain hardening, where it is shown that the composite links with web buckling developed a V_{max} ranging from 1.29 V_y to 1.44 V_y and the bare steel links developing similar values, where V_{max} = 1.38 V_y and 1.44 V_y. Since Specimen A2 did not suffer link web buckling, it was able to achieve V_{max} = 1.53 V_y. M_{max} of the composite links was either approximately equal or greater than M_{max} of the corresponding bare steel links. All specimens developed magnitudes of M_{max} exceeding M_p, as shown in column six of Table 2. Specimen C1 developed the largest magnitude of M_{max}, however, as shown in the seventh column of Table 2 this represents only 0.75 M_{ult}, where M_{ult} is the AISC (Ref.4) flexural capacity based on full composite action.

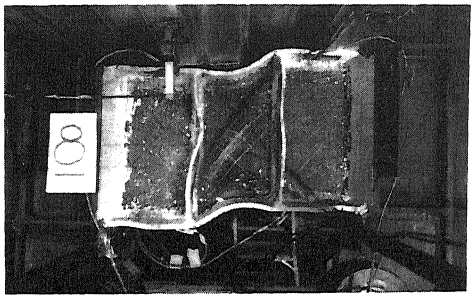

Fig.5 Link of Specimen B1 After Developing Web Buckling in Center Panel.

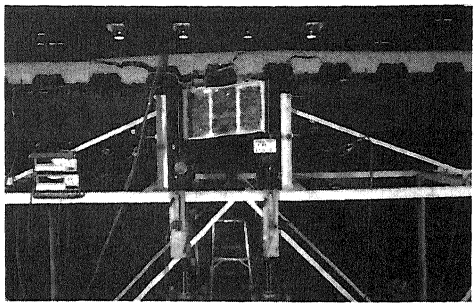

Fig. 6 Floor Slab Damage, Specimen C1.

Specimen [1]	γ_u (rad) [2]	Vmax (kips) [3]	Mmax (kip-in.) [4]	$\frac{V_{max}}{V_y}$ [5]	$\frac{M_{max}}{M_p}$ [6]	$\frac{M_{max}}{M_{ult}}$ [7]
A1	0.079	127.2	1534	1.44	1.29	0.70
B1	0.069	129.2	1369	1.29	1.15	0.61
C1	0.070	118.0	1644	1.36	1.38	0.75
D1	0.073	117.5	1323	1.38	1.11	0.61
A2	–	133.2	1609	1.53	1.35	0.74
B2	0.071	130.7	1500	1.38	1.26	0.66
C2	0.069	120.0	1358	1.40	1.14	0.62
D2	0.076	117.7	1377	1.44	1.16	0.64

Table 2 Maximum Link Forces for Specimens in the (a) K-Braced and, (b) V-Braced Subassemblies.

M_{ult} is not achieved in the links because of the loss of composite action resulting from slab damage. Most of the floor slab damage occurred in the vicinity of the link and consisted primarily of rib cracking, deck separation from the concrete, and slip δ_f between the steel beam and concrete slab due to deformation of the shear connectors. The rib cracking and deck separation is shown in Fig. 6, and the slip δ_f inside the link is compared to δ_f 18 in. outside the link in Fig. 7. The moment-rotation relationship of the floor beam outside the link remained essentially linear, with a change in stiffness under moment reversal, as shown in Fig. 8, where the rotation θ_{ch} of the beam is plotted against moment M. Based on a regression analysis of the experimental data it was determined that for positive moment the effective moment of inertia I_{eff} of the composite floor beam was 2.59I and 1.75I for the interior and exterior floor beams, respectively, where I is the moment of inertia of only the bare steel beam. Under negative moment it was found for all composite beams that I_{eff} = 1.28I. To assess whether the floor slab provided adequate restraint against lateral-torsional buckling of the link, measured histories of the angle of twist ϕ of the steel cross-section at the end of the link were examined. Fig. 9(a) shows a measured history of ϕ at the end of a link with W10 x 15 lateral bracing, and Fig. 9(b) the response of a composite link without lateral bracing. It is apparent from Fig. 9 that the slab does not effectively restrain the steel section against lateral movement, for in Fig. 9(b) the specimen cross-section shows drift from its initial configuration while in Fig. 9(a) the specimen cross-section returns to its initial position.

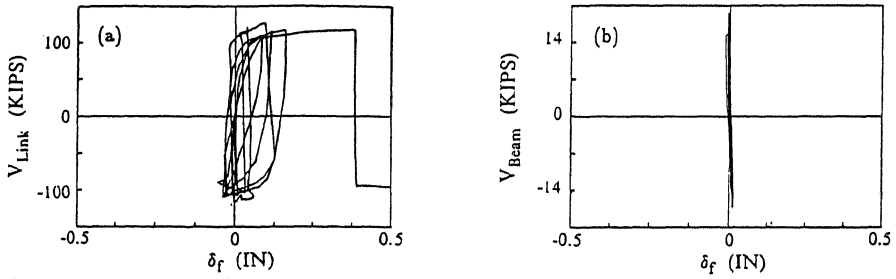

Fig.7 Slip δ_f between Floor Beam and Concrete Slab (a) In the Link, and (b) 18 in. Outside the Link.

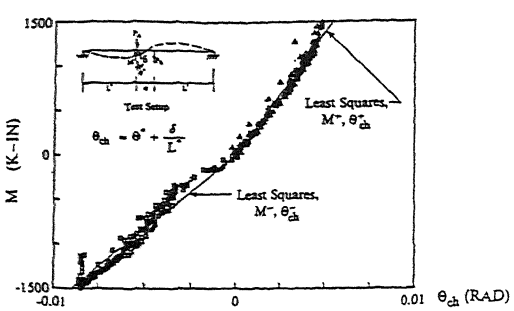

Fig.8 Moment-Rotation Relationship of Composite Floor Beam Outside the Link.

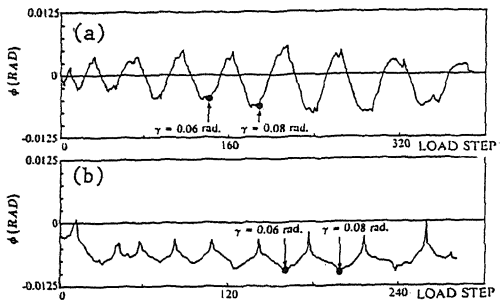

Fig.9 Twist at End of Link for (a) Laterally Braced, and (b) Unbraced Link.

CONCLUSIONS

Based on this limited experimental investigation of the effects of composite action in floors of EBFs, the following tentative conclusions can be reached:

1. Links with composite action have a greater initial elastic stiffness, yield and ultimate strength. Composite links can be designed to yield in shear using current bare steel criteria. The increase in strength should be considered when designing braces and columns adjacent to composite links.
2. Full composite action in the composite links is not maintained during severe cycling due to slab damage. The behavior of the composite floor beam outside the link is essentially linear, for the slab damage is concentrated primarily above the link.
3. Link web buckling occurred in both the bare steel and composite specimens, and can be predicted and controlled using current bare steel link criteria.
4. To maintain ductility of composite links, lateral bracing at the ends of a link must be provided in order to avoid lateral-torsional buckling of the steel beams.

REFERENCES

1. Goel, S.C., and Foutch, D.A., "Preliminary Studies and Test Results of Eccentrically Braced Full-Sized Steel Structure," *U.S.-Japan Cooperative Earthquake Research Program 16th Joint Meeting*, May 15-18, Washington, D.C., 1984.
2. Ricles, J.M., and Popov, E.P., "Experiments on Eccentrically Braced Frames with Composite Floors," *EERC Report No. 87-06*, Earthquake Engineering Research Center, University of California, Berkeley, California, June 1987.
3. *Uniform Building Code*, International Conference of Building Officials, Whittier, California, 1988.
4. *Specification for the Design*, Fabrication and Erection of Structural Steel for Buildings, 8th ed., American Institute of Steel Construction, Chicago, 1980.